Preprints of the 19th World Congress
The International Federation of Automatic Control
Cape Town, South Africa. August 24-29, 2014

Control-Oriented Modeling of A Lithium-Ion Battery for Fast Charging ⋆

Changfu Zou * **Chris Manzie** * **Sohel Anwar** **

* *Department of Mechanical Engineering, University of Melbourne, VIC 3010, Australia (email: changfu.zou@unimelb.edu.au, manziec@unimelb.edu.au)*
** *Department of Mechanical Engineering, Purdue School of Engineering and Technology, IUPUI, Indianapolis, USA (e-mail: soanwar@iupui.edu)*

Abstract: The fast charge battery control problem is characterized by the need to have a sufficiently detailed model that can capture both the charging process and the inevitable constraints that limit the rate of charging due to battery state of health requirements. Presently, it appears the minimal modeling requirements to address the charging problem in model based fashion are unknown. This work seeks to develop a modeling methodology covering a large range of applications through systematically simplifying the partial differential equations that describe battery dynamics. The effects of grid resolution and polynomial order on the complexity and accuracy of reduced order models have been investigated to provide insight into the minimum modeling requirements at different charge rates. The proposed models are intended for controller design and optimization applications including fast charge control.

Keywords: Lithium-ion battery; electrochemical model; reduced-order models; battery fast charge.

1. INTRODUCTION

Partial or full electrification of vehicle powertrain is one approach addressing international expectation of low CO_2 personal transport and high energy efficiency. With this in mind, many studies suggest the proportion of electrified vehicles in the market will significantly increase (e.g. Hensley et al. (2012)). However, the development of electric vehicles (EVs) and hybrid EVs is highly dependent on appropriate use of their key technology, the battery system. Lithium-ion (Li-ion) batteries are considered as the most promising cell chemistry for automotive applications owing to their high energy and power density, no memory effect, and low self-discharge.

The key limiters in EVs uptake currently are the high purchase price, limited range, and charge times compared to internal combustion engine (ICE) vehicles. Price of battery, as a major constituent part of the whole vehicle, is predicted to fall from \$500–\$1000 per kWh today to about \$160–\$300 per kWh by 2025 (Hensley et al. (2012); Kinghorn and Kua (2011)). Range anxiety may be addressed partially through lower battery prices allowing larger packs, but improving the charge rate to an order that allows comparable 'refuel' times with ICE vehicles would also help alleviate range anxiety. Faster charging may also lead to reduced vehicle cost through enabling smaller battery packs. Currently the charge times are limited by the need to conservatively protect the battery state of health (SOH) and lifetime.

Optimal fast charging control involves determining the currents which charge the battery to a given capacity in the shortest time without adversely impacting battery health. The ideal problem can be generally stated in terms of battery dynamics, ω, and the SOH and state of charge (SOC) constraints as:

$$\min_{I(t)} t_f \tag{1a}$$

$$\text{s.t.} \quad \dot{\omega} = f(\omega, t) \tag{1b}$$

$$SOH(t) \geq SOH_{min} \tag{1c}$$

$$SOC(t_f) = SOC_{max} \tag{1d}$$

Model based control has been a successful approach in constraint handling for a range of optimal and sub-optimal control applications, so it is a good candidate for battery management problem, (1). However, a suitable battery model to use in (1b) for fast charge operation which captures the key system characteristics while of reasonable computational complexity is required to achieve this aim. The models of a Li-ion battery widely discussed in the literature can be grouped in two main categories, namely equivalent circuit models (ECMs) and electrochemical models.

ECMs idealize the battery as an open-circuit voltage source connected with several resistors and capacitors, and are typically employed in current battery management system because of low computational times. However, these models are limiting for the lack of detailed battery physical information and low accuracy across a range of

⋆ This work was supported in part by Australia Research Council through grant FT100100538 and Victoria Research Laboratory, National ICT Australia.

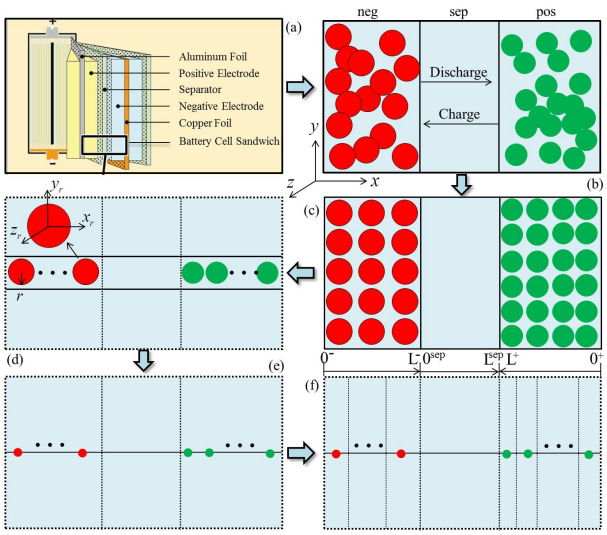

Fig. 1. Schematic and steps to develop a reduced model for a Li-ion cell. a). Infinity dimensional model; b). Full order PDE model; c). 2D PDE model; d). Pseudo 2D (x and r) PDE model; e). 1D PDE model; f). 1D ODE model.

charging conditions and in SOH prediction (Chaturvedi et al. (2010)). Thus, ECMs are not considered here as a suitable structure for (1b).

A first principle model of a Li-ion cell including a lithium-anode, electrolyte and porous insertion cathode was initially presented by Doyle et al. (1993) and reformulated by Chaturvedi et al. (2010). This model structure compromises coupled nonlinear partial differential equations (PDEs) across two spatial dimensions that are impractical for most optimization and control applications, and does not consider temperature variation. Temperature is a particularly important factor in battery modeling because heat generation during charge and discharge is known to potentially have significant impact on the battery's SOH. In view of this, a battery model incorporating coupled electrochemical and thermal behaviors will be proposed in this paper.

Various efforts have been previously made to reformulate and simplify the electrochemical PDE model. Reduced models based on mixed spatial discretization across two dimensions (2D) (e.g. Corno et al. (2012)) show high accuracy relative to the original model, but involve a large system of ordinary differential equations (ODEs). To avoid a large computational burden associated with these models, the authors subsequently propose further simplifications, however these are not, justified analytically or physically, necessarily.

Other simplifications to the spatially discretized model include the use of polynomial profiles and volume-average integration of Li-ion concentration (Subramanian et al. (2001)). Similarly, finite difference methods introduced by Shi et al. (2011) capture electrolyte concentration dynamics, but still exhibit long model computational times due to the large number of nodes present in the model.

A number of other authors have applied model reduction approaches based around elimination of some states or state dynamics (e.g. Klein et al. (2013); Perkins et al. (2012)). The most well known approach is the introduction of the single particle model (SPM) assumption, whereby the positive and negative electrodes and separator are respectively replaced by a single node with lumped parameters and states (Ning and Popov (2004)). These classes of reduced order models all suffer from an inability to suitably capture battery dynamics and SOC/SOH at a wide current range (Santhanagopalan et al. (2006); Moura et al. (2012)). This is clearly an issue in solving the optimal control problem (1).

Consequently, the objective of this work is to establish a library of control-oriented Li-ion cell models with established accuracy over a large range of possible charge rates. The schematic and steps are shown in Fig. 1, starting from the full order electrochemical and thermal PDE model. Model reductions are rigorously applied at each stage, leading to a number of reduced-order model parameters (such as grid resolutions) that must be selected to provide sufficient accuracy at differential charge rates. Simulation studies are performed to provide insight into the parameter requirements for the full range of charge rates considered.

2. PDE MODEL OVERVIEW

In a Li-ion cell, the dynamics (1b) represent the flow of Li-ions from the positive electrode to the negative electrode, and all the resulting electrochemical and thermal phenomena. The starting point for this work will be electrochemical model of Chaturvedi et al. (2010) augmented by the thermal model of Gu and Wang (2000). All later model reductions will have their accuracy measured relative to this initial model formulation.

The key assumptions underpinning the PDE model formulation are as follows:

Assumption 1. Li-ion dynamics along y and z dimensions are negligible.

Remark 1. The implication of this assumption is that Li-ion dynamics are only considered in x dimension and the end effects due to other dimensions are neglected. This is reasonable because the length scales of active material section are typically several orders of magnitude difference between x and the other two dimensions. The simplifying process can be seen in Fig. 1a–c.

Assumption 2. Each agglomeration of lattice sites inside a cell is a spherical solid particle of radius of R_p.

Remark 2. This assumption allows a symmetry argument whereby diffusion in the (x_r, y_r, and z_r) coordinates within a particle can be represented using only r coordinate. Coupled with *Assumption 1*, only x and r coordinates are regarded to fully describe the concentrations in the electrodes.

Assumption 3. There is no direct Li-ion diffusion between adjacent particles.

Remark 3. Li-ion diffusion between adjacent particles is negligible due to the high solid phase diffusive impedance, and thus all kinds of diffusion between particles considered are through the electrolyte.

Assumption 4. The cell consists of active materials and current collectors, and the effects of other components, i.e. tabs, insulator, etc., are not considered. The only heat sources within the cell are reaction heat generation, reversible heat generation, and ohmic heat generation. Heat transport is only caused by internal conductivity and convection between battery surface and ambient.

Remark 4. Thermal models based on this assumption have been experimentally validated by (Gu and Wang (2000)). This allows the rate of temperature change to be written:

$$\rho c\frac{\partial T}{\partial t}=\lambda\frac{\partial^2 T}{\partial x^2}+aFJ(\eta-T\frac{\partial U}{\partial T})-i_e\frac{\partial \Phi_e}{\partial x}-i_s\frac{\partial \Phi_s}{\partial x} \quad (2)$$

where ρ, c, and λ are the density, specific heat, and heat conductivity inside the cell, a and J are the specific interfacial area and molar flux of solid particle, η, i_s, and Φ_s are the overpotential, current, and electric potential in solid particle, F is Faraday's constant, U is open circuit potential, and i_e and Φ_e are the current and potential in electrolyte.

Based on *Assumptions 1-4*, the model shown in Fig. 1d, can now be explicitly described. The dynamic equations in the two electrodes are represented by the same governing equations.

According to Fick's law of diffusion, the Li-ion transport in spherical solid particles and electrolyte are described as

$$\frac{\partial C_s(x,r,t)}{\partial t}=\frac{1}{r^2}\frac{\partial}{\partial r}\left(D_s(T)r^2\frac{\partial C_s(x,r,t)}{\partial r}\right) \quad (3)$$

$$\varepsilon_e\frac{\partial C_e(x,t)}{\partial t}=\frac{\partial}{\partial x}\left(D_e(T)\frac{\partial C_e(x,t)}{\partial x}\right)+\frac{t_-^0}{F}\frac{\partial i_e(x,t)}{\partial x} \quad (4)$$

Based on Ohm's law, the relationship between solid phase potential and current density in solid particles is given by

$$\frac{\partial \Phi_s(x,t)}{\partial x}=-\frac{i_s(x,t)}{\sigma(T)} \quad (5)$$

The variations of potential and current density in electrolyte follow a modified Ohm's law describing the conservation of charge in electrolyte phase, which is

$$\frac{\partial \Phi_e(x,t)}{\partial x}=-\frac{i_e(x,t)}{\kappa(C_e,T)}+\frac{2RT(x,t)t_-^0}{F}\frac{\partial \ln C_e(x,t)}{\partial x} \quad (6)$$

In (3)-(6), t_-^0 is transference number of the cathodes with respect to the solvent velocity, ε_e is volume fraction of the electrolyte, D_e and κ are effective diffusion coefficient and ionic conductivity in the electrolyte, and D_s and σ are effective diffusion coefficient and electronic conductivity in the solid particles.

Considering the Kirchoff's current law, the total current density I through the cross section of a cell is uniform, namely the current density in solid phase and electrolyte satisfy $I(t)=i_s(x,t)+i_e(x,t)$. Due to charge conservation in solid particles, molar flux is determined by the divergence of local electrolyte current

$$\frac{\partial i_e(x,t)}{\partial x}=aFJ(x,t) \quad (7)$$

The above PDEs are coupled by Butler-Volmer Kinetics which describe the relationship among J, η, C_e and C_s (Newman and Thomas-Aleya (2004)).

$$J(x,t)=\frac{i_0(x,t)}{F}\left(e^{\frac{\alpha_a F}{RT(x,t)}\eta(x,t)}-e^{-\frac{\alpha_c F}{RT(x,t)}\eta(x,t)}\right) \quad (8)$$

In (8), α_a and α_c are charge-transfer coefficient of anode and cathode. The overpotential $\eta(x,t)$ and exchange current density $i_0(x,t)$ are modeled as

$$\eta=\Phi_s(x,t)-\Phi_e(x,t)-U(C_{ss}(x,t))-FR_fJ(x,t) \quad (9)$$

$$i_0=r_{eff}C_e(x,t)^{\alpha_a}(C_{s,\max}-C_{ss}(x,t))^{\alpha_a}C_{ss}(x,t)^{\alpha_c} \quad (10)$$

where, C_{ss} is the concentration of Li-ion at the surface of spherical solid particles and is defined as $C_{ss}(x,t)=C_s(x,R_p,t)$. The open circuit potential U is a measured property and is evaluated as an empirical function of C_{ss} by curve-fitting experimental data (Doyle et al. (1996)).

A general thermal model capturing temperature distribution and evolution inside a cell is coupled with the above electrochemical model, and composed of the thermal balance equation and heat generation equation

$$\rho c\frac{\partial T(x,t)}{\partial t}=\lambda\frac{\partial^2 T(x,t)}{\partial x^2}+q(x,t) \quad (11)$$

$$q(x,t)=aFJ(x,t)(\eta(x,t)+T(x,t)\partial U/\partial T)-i_e(x,t)\frac{\partial \Phi_e(x,t)}{\partial x}-i_s(x,t)\frac{\partial \Phi_s(x,t)}{\partial x} \quad (12)$$

In the separator, the governing equations are similar to those for electrodes, but there is no solid particle so that i_s=Φ_s=J=η=0. The complete battery is linked through electrode-separator interfaces that satisfy mass, charge, and energy continuity. For space reason, the boundary conditions required to solve these dynamics equations are not explicitly included, but readers are directed to (Chaturvedi et al. (2010); Gu and Wang (2000)).

In summary, the battery dynamics are represented by (3)-(8) and (11), leading to a set of 17 nonlinear coupled PDEs and algebraic equations. The outputs of interest are the terminal voltage, temperature, SOC, and SOH. The latter two may respectively be expressed as functions of C_{ss} and average Li-ion concentration in solid particles $\bar{C}_s$ (Chaturvedi et al. (2010)); and C_{ss}, $\bar{C}_s$, C_e and η (Ramadass et al. (2004)). The terminal voltage is defined as

$$V(t)=\Phi_s^+(0,t)-\Phi_s^-(0,t) \quad (13)$$

3. MODEL REDUCTION

3.1 Spatial Dimension Reduction

In the 2D model (3)-(12), it is noticed that for each electrode, except Li-ion concentration of solid phase $C_s(x,r,t)$ which involves r coordinate, the other equations are all with respect to x and t. However, the mixed spatial scales result in significant computational overhead, so there is motivation to eliminate the final resolution, r, if possible.

An exact analytical solution of (3) is provided by Carslaw and Jaeger (1973) as

$$C_s(x,r,t)=C_{s0}-\frac{J(x,t)\cdot R_P}{D_s}\left[3\tau+\frac{1}{10}\left(\frac{5r^2}{R_p^2}-3\right)\right]+\frac{2J(x,t)\cdot R_P^2}{D_s r}\sum_{n=1}^{\infty}\frac{\sin(\lambda_n r/R_p)\exp\left(-\lambda_n^2\tau\right)}{\lambda_n^2\sin(\lambda_n)} \quad (14)$$

where, $\tau=D_st/R_P^2$, and $\lambda_j(j=1,2,\dots)$ are the positive eigenvalues of $\lambda_j=\tan(\lambda_j)$.

Equation (14) involves infinite series and is difficult to be directly used for solving the presented battery model. This motivates to find a possible approximation of C_s, expressed as $\hat{C}_s$. On the other hand, to capture battery electrochemical behaviors and predict SOC, the concentration states of interest in each solid particle are the surface concentration, $C_{ss}(x,t)$ and average concentration $\bar{C}_s(x,t)$. With this in mind, an attempt to replace $C_s(x,r,t)$ by $C_{ss}(x,t)$ and $\bar{C}_s(x,t)$ is conducted by assuming:

Assumption 5. At a constant charge rate, $\forall \varepsilon > 0, \exists n(\varepsilon, I) \in \mathbb{Z}$ satisfying $||C_s(x,r,t) - \hat{C}_{s,n}(x,r,t)||_2 < \varepsilon$.

Remark 5. A solution for $\hat{C}_{s,n}(x,r,t)$ was obtained by approximating the solid phase Li-ion concentration with the following polynomial form (Subramanian et al. (2001))

$$\hat{C}_{s,n}(x,r,t) = a_1(x,t) + a_2(x,t)\frac{r^2}{R_P^2} + \cdots + a_n(x,t)\frac{r^{2n}}{R_P^{2n}} \tag{15}$$

By substituting (15) into (3) and employing volume-average integration of r, the 2D second-order PDE, (3) in each electrode can be decoupled to a first-order PDE and an algebraic equation in terms of $C_{ss}(x,t)$ and $\bar{C}_s(x,t)$, which are given as

$$\partial \bar{C}_s(x,t)/\partial t = -3J(x,t)/R_P \tag{16}$$

$$C_{ss}(x,t) = C_{s0} - J(x,t)\cdot R_P(3\tau + 0.2)/D_s + \frac{J(x,t)\cdot R_P}{D_s}\sum_{n=1}^{\infty}\frac{2\exp\left(-\lambda_n^2\tau\right)}{\lambda_n^2} \tag{17}$$

For convenience, we define $\vartheta(x,t)=J(x,t)R_P/D_s$. Through utilizing the second, fourth, and sixth-order polynomials for (15), equation (17) can be further approximated by (Subramanian et al. (2001))

$$C_{ss,1}(x,t) = C_{s0} - \vartheta(x,t)(3\tau + 0.2) \tag{18}$$

$$C_{ss,2}(x,t) = C_{s0} - \vartheta(x,t)\left(3\tau + 0.2 - 2e^{-35\tau}/35\right) \tag{19}$$

$$C_{ss,3}(x,t) = C_{s0} - \vartheta(x,t)\left(3\tau + 0.2 - 0.1135e^{-100.123\tau}\right) + \vartheta(x,t)\left(0.0864e^{-18.877\tau}\right) \tag{20}$$

It is worth mentioning that the polynomial order, n is "tuning parameter" for these polynomial approximations to reflect concentration dynamics. The accuracy and application of battery models yielded by different order polynomials will be investigated in the next section.

3.2 Spatial Discretization

A further model simplification is possible by approximating the 1D PDE model of (4)-(8), (11), (16) and (17) by ODEs. This can be realized by finite difference through discretizing each domain (l^-, l^+ and l^{sep}) in a cell to N elements with grid resolution Δx_i. In each element, all states are assumed to be uniform. In this way, a discretized battery model with uniform resolution is given by

$$d\bar{C}_s(i)/dt = -3J(i)/R_P \tag{21}$$

$$C_{ss,n}(i) := C_s(i, R_p) \tag{22}$$

$$\varepsilon_e\frac{dC_e(i)}{dt} = D_e\frac{C_e(i+1) - 2C_e(i) + C_e(i-1)}{(\Delta x)^2} + t_-^0(i_e(i+1) - i_e(i))/(F\Delta x) \tag{23}$$

$$(\Phi_s(i+1) - \Phi_s(i))/\Delta x = -i_s(i)/\sigma(i) \tag{24}$$

$$(\Phi_e(i+1) - \Phi_e(i))/\Delta x = -i_e(i)/\kappa(i) + \frac{2RT(i)t_-^0}{F}\frac{\ln C_e(i+1) - \ln C_e(i)}{\Delta x} \tag{25}$$

$$(i_e(i+1) - i_e(i))/\Delta x = aFJ(i) \tag{26}$$

$$J(i) = \frac{i_0(i)}{F}\left(e^{\frac{\alpha_a F\eta(i)}{RT(i)}} - e^{-\frac{\alpha_c F\eta(i)}{RT(i)}}\right) \tag{27}$$

$$\rho c\frac{dT(i)}{dt} = \lambda\frac{T(i+1) - 2T(i) + T(i-1)}{(\Delta x)^2} + aFJ(i)(\eta(i) + T(i)\partial U/\partial T) - i_e(i)\frac{\Phi_e(i+1) - \Phi_e(i)}{\Delta x} - i_s(i)\frac{\Phi_s(i+1) - \Phi_s(i)}{\Delta x} \tag{28}$$

Here i denotes the i-th element in each electrode or separator. In conjunction with the discretized expressions of (10), (11) and corresponding boundary conditions, the PDE battery model is approximated by a spatial discretized model that includes $8N$ ODEs and $11N$ algebraic equations (AEs) associated with $19N$ states in the entire battery region, as shown in Fig. 1f. To investigate the applications of this proposed model at different charge rates, N is "tuning parameter".

Typical battery parameters like those observed in (Doyle et al. (1996); Gu and Wang (2000)) lead to separation of length scales between some states in (21)-(28). To capture this effect, the $19N$ state equations will be considered with different level of discretization, particularly focusing on the temperature and electric potential. This leads to $14N+2N_\Phi+N_T$ total equations, with now three discretization variables to be considered.

4. SIMULATION RESULTS

One of the typical methods to validate a cell model is using constant current charge and discharge at different current rates (Chaturvedi et al. (2010)). In this paper, to evaluate the proposed models over the entire possible operating domain, the inputs are constant currents ranging from 0.5C to 10C. The ambient temperature and initial battery temperature are both set at 25°C. The cell parameters are taken from (Doyle et al. (1996); Gu and Wang (2000)) and they are related to a prismatic $LiMnO_4/LiC_6$ battery.

The PDE model (3)-(12) is solved by COMSOL Multiphysics 4.3a. While, the proposed model (21)-(28) for a given (N, N_{Φ_s}, N_T and n) set is solved by DASSL under the same conditions. During each cycle, fully charged Li-ion cells are discharged from 4.2V to 2.8V using both models. The terminal voltages sampled at 10 Hz, leading to V_k and $\bar{V}_k$ for the proposed model and PDE model, respectively. The normalized root-mean-square (RMS) error in voltage estimation is consequently defined as

$$\beta := \sqrt{\frac{\sum_1^M\left(V_k - \bar{V}_k\right)^2}{M}}\Big/\frac{\sum_1^M \bar{V}_k}{M} \times 100\%$$

4.1 Minimal States of Electric Potential, N_Φ

The electric potential gradient in solid particles is examined with a view to determining the minimal N_{Φ_s} at various charge rates. Define the discretized spatial approximation of Φ_s and the resulting approximation error as:

$$\Phi_s^d(i,t) := \frac{N_\Phi}{l}\int_{il/N_\Phi}^{(i+1)l/N_\Phi} \Phi_s(x,t)dx, x \in [i, i+1]\,\frac{l}{N_\Phi} \quad (29)$$

$$\Delta\Phi_s(x,t) := \Phi_s(x,t) - \Phi_s^d(i,t), \forall i \in [1, N_\Phi] \cap \mathbb{Z} \quad (30)$$

Lemma 1. The discretized Φ_s^d model with N_Φ satisfies

$$|\Delta\Phi_s(x,t)| \leq \varepsilon_\Phi \quad (31)$$

and $\varepsilon_\Phi := I(t)l/\sigma N_\Phi$, where σ represents the minimum value of $\sigma(T)$ (at initial temperature).

Proof 1. From equation (5), Φ_s is monotonic in x, such that the error in any given element $[i, i+1]\,l/N_\Phi$ is

$$|\Delta\Phi_s(x,t)| \leq |\Phi_s\left((i+1)l/N_\Phi\right) - \Phi_s\left(il/N_\Phi\right)| \quad (32)$$

By integration on both sides of (5) across one element, we obtain

$$\int_{il/N_\Phi}^{(i+1)l/N_\Phi} \frac{\partial\Phi_s(x,t)}{\partial x}dx = \int_{il/N_\Phi}^{(i+1)l/N_\Phi} -\frac{i_s(x,t)}{\sigma(T)}dx$$

$$\varepsilon_\Phi^i := |\Phi_s\left((i+1)l/N_\Phi, t\right) - \Phi_s\left(il/N_\Phi, t\right)|$$

$$= \left|\int_{il/N_\Phi}^{(i+1)l/N_\Phi} \frac{i_s(x,t)}{\sigma(T)}dx\right| \leq \left|\frac{I(t)l}{\sigma N_\Phi}\right| \quad (33)$$

So, $\varepsilon_\Phi := \max_i \varepsilon_\Phi^i = I(t)l/(\sigma N_\Phi)$.

Remark 6. Using typical battery parameters of (Doyle et al. (1996)) and considering 10C operation rate, the error in the negative electrode is bounded by $N_\Phi\varepsilon_\Phi^- \leq 0.541$mV, which corresponds to a relative error 0.06%. Consequently, the choice $N_\Phi^-=1$ seems reasonable. Conversely, in the positive electrode the reduced conductivity relative to the negative electrode leads to $N_\Phi\varepsilon_\Phi^+ \leq 53.96$mV, on a relative error 1.324%. To ensure high accuracy of the electric potential in this electrode, N_Φ^+ is chosen to be N.

Remark 7. Inaccuracies in Φ_s can also potentially impact other states through the coupled dynamics evident in (9) and (11). However, a first order Taylor series expansion of these equations with perturbed Φ_s exhibits only negligible effect on η and T for realistic parameter values.

4.2 Minimal Temperature States, N_T

The thermal phenomena is heavily coupled with electrochemical reactions governed by (3)-(12), so it is impractical to obtain ε_T by analytical deduction in a way similar to Section 4.1. In light of this, the temperature distribution along x coordinate in an electrode pair can be derived by simulations based on the PDE model. To gain the temperature profile across an entire cell, which consists of L/l electrode pairs, the heat generation rate is assumed to be uniform (Muratori et al. (2000)) and scaled by $q(t)L/l$. The typical heat transfer coefficient (h) between the cell and ambient can be: 5W/m^2·K (normal convection); 30 or 100W/m^2·K (forced convection). To explore the extreme temperature difference between battery surface and center, h is chosen to be 100, and the resulting cell temperature profiles at different current rates are shown in Fig. 2.

It is apparent that the peak temperature difference in the cell is bounded by $\Delta T \leq 4$K, which corresponds to a relative error $\Delta T/\bar{T}$ 1.24%. Moreover, the lower h and current rate are adopted, the smaller error will be obtained. After also confirming negligible coupling effects in parameters D_s, D_e, σ and κ, and states J, at this scale of temperature error, the temperature gradient in the cell is evidently negligible, and a good approximation can be therefore achieved by the lumped parameter approach with N_T=1, $T(x,t)$=$T(t)$.

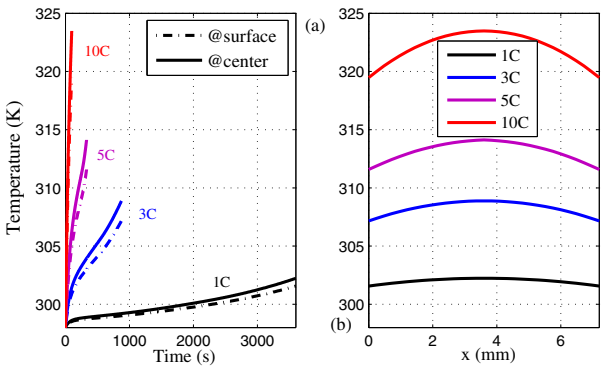

Fig. 2. Temperature profiles in a battery cell at 1, 3, 5, and 10C discharge operations. (a). Temperature variation at battery surface (solid) and center (dashed); (b). Temperature distribution across battery thickness direction at the end of discharge operation (2.8V). The heat transfer coefficient and thermal conductivity are h=100W/m^2·K, λ=0.99W/m·K.

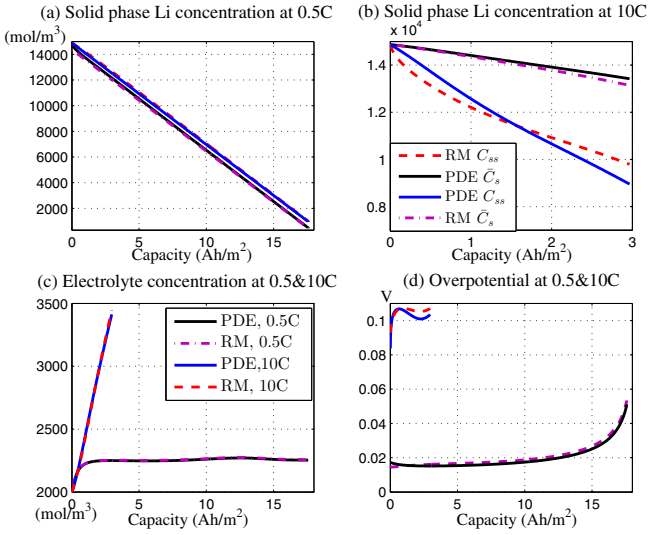

Fig. 3. Comparison of the reduced model (RM) and PDE model in terms of C_{ss}, $\bar{C}_s$, C_e, and η (at current collector) during 0.5C and 10C charge operations. For 0.5C, n=N=1; for 10C, n=3 and N=10.

4.3 Minimal Resolution of Remaining State, N

Having reduced the parameters N_T=N_Φ^-=1, the modeling complexity is fully stated in terms of N and n. These parameters determine the ability of the reduced order model to reproduce the outputs of full PDE model to a given accuracy level. Specifying the accuracy levels of interest to be β=5% (for closed loop control) and β=1% (for open loop optimization), the minimal N and n were found over a range of charge rates and given in Table 1.

The accuracy of the single particle model represented by N=1 is limited to low charge rates as previously observed in the literature (e.g. Santhanagopalan et al. (2006)). For

Table 1. Appropriate polynomial profile and grid resolution for different charge rates.

	Requirements for β <5%					Requirements for β <1%				
Rate	n	N	N_T	N_Φ^-	β	n	N	N_T	N_Φ^-	β
0.5C	1	1	1	1	0.39	1	1	1	1	0.39
1C	1	1	1	1	0.87	1	1	1	1	0.87
2C	1	1	1	1	1.97	1	3	1	1	0.73
3C	2	1	1	1	3.30	2	2	1	1	0.83
4C	2	1	1	1	4.79	2	5	1	1	0.94
5C	2	2	1	1	3.13	3	5	1	1	0.93
6C	3	2	1	1	1.56	3	6	1	1	0.99
7C	3	2	1	1	1.66	3	7	1	1	1.00
8C	3	2	1	1	1.80	3	8	1	1	0.96
9C	3	2	1	1	2.04	3	9	1	1	0.98
10C	3	2	1	1	2.38	3	10	1	1	0.99

charge rates >1C, to maintain model accuracy of 1%, increasing N and n are required. Reducing the accuracy requirement to 5% means the single particle model maintains its ability to 4C rates. For high charge/discharge rates, the complexity requirements increase monotonically with current. For fast charge optimization problems, this potentially means models with up to 10 spatial states and 6th order polynomial approximation must be used. The significance of this increased modeling request can be expressed in terms of the computational load differences. The N=10, n=3 set up is 10 times slower than the N=1, n=1, but still 500 times faster compared to the PDE model.

So far, the output voltage and temperature of the PDE model is well approximated by a library of models consisting of $5N$+1 ODEs and $10N$+1 AEs. As stated earlier, based on the prevalent literature, SOC and SOH are functions of the internal states, C_{ss}, $\bar{C}_s$, C_e, and η. The capability of the reduced models presented in Table 1 to capture these states at different charge rates is examined and shown in Fig. 3. It can be seen that close agreement is achieved for the upper and lower bounds of the considered current range. If SOC and SOH are well-captured by these states, then the proposed models are therefore capable in dealing with the constraints on problem (1).

5. CONCLUSION

The coupled electrochemical and thermal battery models presented in this paper consist of a 1D ODAE system and are derived from the PDE model with the use of several simplifying assumptions, finite difference method, polynomial approximation, and volume-average integration. The requirements for the proposed model to achieve given modeling accuracy from 0.5C to 10C charge rates were found using a combination of theoretical analysis and simulations to identify the minimal parameter set (N, n, N_Φ and N_T). The proposed models exhibit significantly reduced computational times relative to the PDE model. Future work will concentrate on using these models in the solution of the optimal fast charge problem (1).

REFERENCES

Carslaw, H.S. and Jaeger, J.C. Conduction of Heat in Solids. page 112, *Oxford University Press*, London, 1973.

Chaturvedi, N., Klein, R., Christensen, J., Ahmed, J., and Kojic, A. Algorithms for advanced battery management systems: modeling, estimation, and control challenges for lithium-ion batteries. *IEEE Control Systems Magazine*, vol. 30(3), 2010.

Corno, M., Bhatt, N., and Verhaegen, M. An efficient control oriented modeling approach for lithium ion cells. *American Control Conference*, Canada, 2012.

Doyle, M., Fuller, T.E., and J. Newman. Modeling of galvanostatic charge and discharge of the lithium/polymer/insertion cell. *Electrochemical Science and Technology*, vol. 140(6), pages 1526–1533, 1993.

Doyle, M., Newman, J., Gozdz, A.S., Schmutz, C.N., and Tarascon, J.M. Comparison of modeling predictions with experimental data from plastic lithium ion cells. *Journal of The Electrochemical Society*, vol. 143, pages 1890–1903, 1996.

Gu, W.B. and Wang, C.Y. Thermal and electrochemical coupled modeling of a lithium-ion cell in lithium batteries. *ECS Proceedings*, vol. 99–25(1), pages 748–762, 2000.

Hensley, R., Newman, J., and Rogers, M. Battery technology charges ahead. *Mckinsy Quarterly*, July 2012.

Kinghorn, R. and Kua, D. Forecast Uptake and Economic Evaluation of Electric Vehicles in Victoria. *Technical Report*. page 18, May 2011.

Klein, R., Chaturvedi, N.A., Christensen, J., Ahmed, J., Findeisen, R., and Kojic, A. Electrochemical model based observer design for a lithium-ion battery. *IEEE Transactions On Control Systems Technology*, vol. 21, pages 289–302, 2013.

Moura, S.J., Chaturvedi, N.A., and Krstic, M. Adaptive PDE observer for battery SOC/SOH estimation. *ASME Dynamic Systems and Control Conference*, Ft. Lauderdale, FL, 2012.

Muratori, M., Canova, M., Guezennec, Y., and Rizzoni, G. A reduced-order model for the thermal dynamics of Li-Ion battery cells. *IFAC Symposium Advances in Automotive Control*, Munich, Germany, July, 2010.

Newman, J. and Thomas-Aleya, K.E. Electrochemical Systems. 3rd ed., *John Wiley & Sons Inc*, 2004.

Ning, G. and Popov, B.N. Cycle life modeling of lithium-ion batteries. *Journal of The Electrochemical Society*, vol. 151(10), pages A1584A1591, 2004.

Perkins, R.D., Randall, A.V., Zhang, X., and Plett, G.L. Controls oriented reduced order modeling of lithium deposition on overcharge. *Journal of Power Sources*, vol. 209, pages 318–325, 2012.

Ramadass, P., Haran, B., Gomadam, P.M., White, R., and Popov, B.N. Development of first principles capacity fade model for Li-Ion cells. *Journal of The Electrochemical Society*, vol. 151(2) pages A196-A203, 2004.

Santhanagopalan, S., Guo, Q., Ramadass, P., and White, R.E. Review of models for predicting the cycling performance of lithium ion batteries. *Journal of Power Sources*, vol. 156, pages 620–628, 2006.

Shi, Y., Prasad, G., Shen. Z., and Rahn, C.D. Discretization methods for battery systems modeling. *American Control Conference*, San Francisco, CA, USA, pages 356–361, 2011.

Subramanian, V.R., Ritter, J.A., and White, R.E. Approximate solutions for galvanostatic discharge of spherical particles -1. Constant diffusion coefficient. *Journal of The Electrochemical Society*, vol. 148(11), pages E444–E449, 2001.